RESEARCH PAPER

Benzofuran analogues of amphetamine and methamphetamine: studies on the metabolism and toxicological analysis of 5-APB and 5-MAPB in urine and plasma using GC-MS and LC-(HR)-MS^n techniques

Jessica Welter · Pierce Kavanagh · Markus R. Meyer ·
Hans H. Maurer

Abstract 5-APB (5-(2-aminopropyl)benzofuran) and its *N*-methyl derivative 5-MAPB (*N*-methyl-5-(2-aminopropyl)benzofuran) are analogues of amphetamine and methamphetamine, respectively, and belong to the so-called novel psychoactive substances (NPS). They were consumed as stimulants or entactogens with euphoric and empathogenic effects. Being controlled in some countries, both compounds should be covered by drug testing in clinical and forensic toxicology. Therefore, metabolism studies have been performed by working up rat urine samples after a high single dose of the corresponding NPS with solid-phase extraction without and after enzymatic conjugates cleavage. The phase I metabolites were separated and identified after acetylation by GC-MS and/or LC-HR-MS^n and the phase II metabolites by LC-HR-MS^n. The main metabolite of 5-APB was 3-carboxymethyl-4-hydroxy amphetamine and the main metabolites of 5-MAPB were 5-APB (*N*-demethyl metabolite) and 3-carboxymethyl-4-hydroxy methamphetamine. The cytochrome P450 (CYP) isoenzymes involved in the 5-MAPB *N*-demethylation were CYP1A2, CYP2B6, CYP2C19, and CYP2D6, and according to the kinetic parameters, CYP2B6 was responsible for the main part of the total CYP-dependent clearance. An intake of a common users' dose of 5-APB or 5-MAPB could be confirmed in rat urine using the authors' GC-MS and the LC-MS^n standard urine screening approaches with the corresponding parent drugs as major target. In authentic human urine samples after ingestion of unknown doses of 5-MAPB, both metabolites could also be detected besides the parent drug. The plasma concentrations determined in six clinical cases ranged from 5 to 124 μg/L for 5-MAPB and from 1 to 38 μg/L for its *N*-demethyl metabolite 5-APB.

Keywords 5-APB · 5-MAPB · Metabolism · Plasma concentration · GC-MS · LC-(HR)-MS^n

Introduction

5-APB (5-(2-aminopropyl)benzofuran) and its *N*-methyl derivative 5-MAPB (*N*-methyl-5-(2-aminopropyl)benzofuran) are benzofuran analogues of amphetamine and methamphetamine, respectively, and belong to the so-called novel psychoactive substances (NPS). Considering the benzofuran ring, they are also MDA (3,4-methylenedioxy-amphetamine) and MDMA (3,4-methylendioxy-methamphetamine) analogues with bioisosteric substitution of one oxygen (–O–) in the furan ring by methine (–CH=). These compounds are sold as so-called "research chemicals" via the internet. They appeared first in 2010 and 2012, respectively, when users on internet drug forums (e.g., www.bluelight.org; www.land-der-traeume.de) started to discuss their effects. They are consumed as stimulating or entactogenic drugs with euphoric and empathogenic effects similar to those of MDA and MDMA. Discussed negative effects were typical for stimulants, such as tachycardia, jaw tension, hyperthermia, insomnia, and anxiety [1]. Iversen et al. investigated the effects and binding activities of 5-APB on different transporters and receptors [2]. They found that 5-APB has inhibitory effects on the dopamine (DA), noradrenalin (NA), and

J. Welter · M. R. Meyer · H. H. Maurer (✉)
Department of Experimental and Clinical Toxicology, Institute of Experimental and Clinical Pharmacology and Toxicology, Saarland University, 66421 Homburg, Saar, Germany
e-mail: hans.maurer@uks.eu

P. Kavanagh
Department of Pharmacology and Therapeutics, Trinity Centre for Health and Sciences, St. James's Hospital, Dublin 8, Ireland

🕿 Springer

serotonin (5-HT) reuptake transporters with potencies similar to amphetamine but with higher potency on the 5-HT transporter. Furthermore, 5-APB showed high binding affinity on the 5-HT$_{2B}$ receptor and was confirmed as potent full agonist. In addition, Dawson et al. showed that 5-APB bound to the DA transporter blocking the reuptake and increased in higher concentrations the level of basal DA comparable to amphetamine and thus claimed to be a modest amphetamine-type stimulant (ATS) [3]. They also found 5-APB being an agonist at the 5-HT$_{2A}$ and 5-HT$_{2B}$ receptor. These results might explain the described vasoconstrictive, stimulating, and hallucinogenic effects. Unfortunately, the effects of 5-MAPB have not been elucidated but might be similar considering structure analogy and the pharmacological effects described by users.

5-APB is controlled in Germany, both compounds in the UK, and in several other countries they were controlled by analogue acts. Nevertheless, they are still commercially available on the internet. So far, only few data on analytics of 5-APB and 5-MAPB are available. Stanczuk et al. investigated the differentiation of the positional isomers of APB in purchased products. They could separate them by gas chromatography–mass spectrometry (GC-MS) after heptafluorobutyrylation [4]. Casale et al. also differentiated between the several positional isomers by GC-MS but without derivatization [5]. To date, no data was published on their metabolism or detectability in biosamples, and thus, the aims of this work were to identify their phase I and II metabolites in rat urine by GC-MS and liquid chromatography–high-resolution linear ion trap mass spectrometry (LC-HR-MS^n) and to investigate the human cytochrome P450 (CYP) isoenzymes involved in the main metabolic steps with calculation of the corresponding kinetic constants. Another aim was to study the detectability of a common users' dose in rat urine by the GC-MS [6] and liquid chromatography–linear ion trap mass spectrometry (LC-MS^n) [7, 8] standard urine screening approaches (SUSAs). Finally, detection in urine and quantification of 5-MAPB and 5-APB in plasma of authentic 5-MAPB cases should be investigated.

Experimental

Chemicals and reagents

5-APB and 5-MAPB were synthesized [4] and provided by the Department of Pharmacology and Therapeutics, Trinity Centre for Health Sciences, St. James's Hospital (Dublin, Ireland), before scheduling. Isolute C18 (500 mg, 3 mL) and HCX cartridges (130 mg, 3 mL) were obtained from Biotage (Uppsala, Sweden); MDMA and MDMA-d$_5$ from LGC (Wesel, Germany); isocitrate and isocitrate dehydrogenase, heptafluorobutyric anhydride, and sodium phosphate from Sigma-Aldrich (Taufkirchen, Germany); NADP$^+$ from Biomol (Hamburg, Germany); acetonitrile (LC-MS grade),

ammonium formate (analytical grade), formic acid (LC-MS grade), methanol (LC-MS grade), and mixture (100,000 Fishman units/mL) of glucuronidase (EC No. 3.2.1.31) and arylsulfatase (EC No. 3.1.6.1) from Helix Pomatia; and all other chemicals and reagents (analytical grade) from VWR (Darmstadt, Germany). The baculovirus-infected insect cell microsomes (ICM; Supersomes) containing 1 nmol/mL of human cDNA-expressed CYP1A2, CYP2A6, CYP2B6, CYP2C8, CYP2C9, CYP2C19, CYP2D6, CYP2E1 (2 nmol/mL), CYP3A4, or CYP3A5 (2 nmol/mL), and pooled human liver microsomes (pHLM, 20 mg microsomal protein/mL, 400 pmol total CYP/mg protein) were obtained from BD Biosciences (Heidelberg, Germany). After delivery, the microsomes were thawed at 37 °C, aliquoted, snap-frozen in liquid nitrogen, and stored at −80 °C until use.

Urine samples

Urine samples from male Wistar rats (Charles River, Sulzfeld, Germany) were used after administration of the compounds by gastric intubation using an aqueous suspension for toxicological diagnostic reasons according to the corresponding German law (http://www.gesetze-im-internet.de/tierschg/). For identification of the metabolites, a single 20 mg/kg body mass (BM) dose for 5-APB and 5-MAPB and for toxicological analysis, a single 3 mg/kg BM dose for 5-APB or 1 mg/kg BM dose for 5-MAPB were administered once. The rats were housed in metabolism cages for 24 h, having water ad libitum. Urine was collected separately from the feces over a 24-h period. Blank urine samples were collected before drug administration to check whether the samples were free of interfering compounds. The samples were directly analyzed and then stored at −20 °C. Human urine samples from authentic cases after suspected intake of 5-MAPB or other NPS, submitted to the authors' laboratory for emergency toxicological reasons, were also analyzed.

Sample preparation for identification of phase I and II metabolites

As described previously [9], urine samples were extracted after conjugate cleavage with a mixture of glucuronidase and arylsulfatase by solid-phase extraction (SPE) with HCX cartridges. After elution, evaporation, and reconstitution in 100 μL of methanol, 50 μL was left underivatized and another 50 μL was again gently evaporated to dryness and derivatized with a mixture of acetic anhydride and pyridine (3:2 v/v) under microwave irradiation. Afterwards, the residue was reconstituted in 50 μL of methanol. A 1-μL aliquot of the extract was injected onto the GC-MS or 5 μL onto the LC-HR-MS^n.

For the phase II metabolism studies, 1 mL of urine was extracted by SPE (C18). A 5-μL aliquot of the extract was injected onto the LC-HR-MS^n.

GC-MS apparatus for identification of the phase I metabolites

A Hewlett Packard (HP, Agilent, Waldbronn, Germany) 6890 Series gas chromatograph combined with an HP 6890 MSD mass spectrometer and an HP MS ChemStation (DOS series) with HP G1701AA software version A03.00 was used for analysis of the extracts. The GC conditions were as follows: splitless injection mode; column, Optima 5 MS capillary (12 m×0.2 mm I.D.), cross-linked methyl silicone, 0.35 μm film thickness (Macherey-Nagel, Düren, Germany); injection port temperature, 280 °C; carrier gas, helium; flow rate, 0.5 mL/min; column temperature, programmed from 85 to 310 °C at 30 °C/min, initial time 2 min, final time 7 min, total time 16 min. The MS conditions were as follows: full-scan mode, m/z 50–550 u; electron ionization (EI) mode, ionization energy, 70 eV; ion source temperature, 220 °C; capillary direct interface, heated at 280 °C.

LC-HR-MS^n apparatus for identification of phase I and II metabolites

For analysis of the prepared extracts, the same system as described previously [9] was used: Thermo Fisher Scientific (TF, Dreieich, Germany) Dionex UltiMate 3000 RS pump consisting of a degasser, a quaternary pump, and an UltiMate 3000 RS autosampler, coupled to a TF Orbitrap Velos Pro equipped with a heated electrospray ionization (HESI) II source. For details of the LC and MS conditions, see Ref. [9]. Briefly, a TF Hypersil Gold column (150×2.1 mm, 1.9 μm) with gradient elution with 10 mM aqueous ammonium formate buffer containing 0.1 % (v/v) formic acid as mobile phase A and acetonitrile containing 0.1 % (v/v) formic acid as mobile phase B was applied. The Orbitrap (OT) was run in the positive mode and the collision-induced dissociation (CID)–MS/MS experiments (normalized collision energies, 35 %) were either performed in a data-dependent scan mode (m/z 100–800) or on the following selected precursor ions from MS^1 at m/z 176 and 190 for the underivatized parent compounds and 218, 232, 276, 278, 290, 292, 294, 296, 308, 322, 336, and 394 for the acetylated parent compounds and phase I metabolites, as well as 372, 386, and 400 for phase II metabolites.

LC-HR-MS/MS apparatus for analysis of the microsomal incubation and kinetics

A TF Accela LC system consisting of a degasser, a quaternary pump, and a HTC PAL autosampler (CTC Analytics, Zwingen, Switzerland) coupled to a TF Q-Exactive system equipped with an HESI-II source was used. The instrument was mass calibrated prior to analysis infusing a Positive Mode Cal Mix (Supelco, Bellefonte, PA) at a flow rate of 5 μL/min using a syringe pump. The LC and MS conditions were as described elsewhere [10]: TF Accucore PhenylHexyl column (150×2.1 mm, 2.6 μm); gradient elution with Millipore water containing formic acid (0.1 % v/v, pH 3) as mobile phase A and acetonitrile containing formic acid (0.1 %, v/v) as mobile phase B. The gradient and flow rate were programmed as described previously [10]. The MS conditions for the initial screening studies were as follows: scan experiment 1 was in targeted MS^2 mode with an inclusion list containing the m/z for 5-APB, hydroxy, hydroxy-dihydro, 3-carboxymethyl-4-hydroxy amphetamine (m/z 176.1069, 192.1019, 194.1175, 210.1124) or 5-MAPB, N-demethyl, hydroxy, hydroxy-dihydro, and 3-carboxymethyl-4-hydroxy methamphetamine (m/z 176.1069, 190.1226, 206.1175, 208.1332, 224.1281); positive scan mode; resolution, 35,000; automatic gain control (AGC) target, 5e5; maximum injection time (IT) 250 ms; normalized collision energy (NCE) at 35 eV. Scan experiment 2 was a full MS in positive scan mode from m/z 50 to 500, resolution, 17,500; AGC, 1e6; IT, 120 ms. For the kinetic studies, a targeted selected-ion monitoring mode (t-SIM) was used with the m/z for 5-MAPB, N-demethyl 5-MAPB, and MDMA as internal standard (m/z 176, 190, 194). The settings for the t-SIM mode with an inclusion list were as follows: resolution, 17,500; microscans, 1; AGC, 1e6; IT, 250 ms; MSX count, 3; isolation width, 1; scan range, m/z 100 to 200. TF Xcalibur Qual Browser software version 2.2 SP1.48 was used for calculation of the peak areas for assessment of the amount of 5-APB formed during incubation. TF Xcalibur Qual Browser software version 2.2 SP1.48 was used for calculation of the peak areas ratios (analyte vs. IS) for assessment of the amount of metabolites formed during incubation using a freshly prepared calibration of 5-APB (concentration between 0.001 and 10 μmol/L).

Microsomal incubations for HLM and initial CYP activity screening studies

Conditions for the performance of the microsomal incubations for each isomer were published before [11]. Briefly, the drugs (150 μmol/L each) were incubated with the CYP isoenzymes (50 pmol/mL, each) CYP1A2, CYP2A6, CYP2B6, CYP2C8, CYP2C9, CYP2C19, CYP2D6, CYP2E1, CYP3A4, CYP3A5, or HLM (1 mg protein/mL) for 30 min. After incubation, the solution was centrifuged, the supernatant transferred to an autosampler vial, and 10 μL injected onto the LC-HR-MS/MS.

Enzyme kinetic studies

For the calculation of kinetic constants of the N-demethylation step of 5-MAPB, the incubation conditions were chosen to be within linear range of metabolite formation. Incubation time was 10 min for HLM and CYP1A2, 5 min for CYP2B6, and 20 min for CYP2C19. The protein concentration was 30 pmol/mL for the CYP incubations and 0.8 mg/mL for HLM

incubations. The used substrate concentrations for HLM as well as the CYP isoenzymes were 1, 10, 50, 100, 250, 500, 750, 1000, 1500, and 2000 µmol/L. Enzyme kinetic constants were estimated by nonlinear curve fitting using the GraphPad Prism 5.00 software (San Diego, CA). The Michaelis–Menten equation [Eq. (1)] was used to calculate apparent K_m (Michaelis–Menten constant) and V_{max} (maximum velocity) values for single-enzyme systems and HLM.

$$V = \frac{V_{max*}[S]}{K_m + [S]} \tag{1}$$

Calculation of relative activity factors, contributions, and percentages of net clearance

To consider the different functional levels of redox partners between two different enzyme sources, the relative activity factor (RAF) approach [12–14] was used. The turnover rates of the specific probe substrates (PS) in the used batches of ICM and pHLM were taken from the supplier's data sheets and used for calculation of the RAFs according to Eq. (2): CYP1A2 (PS phenacetin), CYP2C19 (PS S-mephenytoin), CYP2D6 (PS bufuralol), and CYP2B6 (PS S-mephenytoin).

$$RAF_{enzyme} = \frac{TR_{PS} \, in \, HLM(pmol/min/mg \, protein)}{TR_{PS} \, in \, ICM(pmol/min/mg \, protein)} \tag{2}$$

To calculate the contribution, the corresponding RAFs were multiplied with the enzyme velocities V_{enyzme} for the respective metabolic reactions at different substrate concentrations according to Eq. (3).

$$contribution_{enzyme} = RAF_{enzyme} * V_{enzyme} \tag{3}$$

The percentages of net clearance by a particular P450 at a certain substrate concentration can be calculated from these corrected activities (contributions) according to Eq. (4), where clearance equals contribution/K_m:

$$clearance_{enzyme}[\%] = \frac{clearance_{enzyme}}{\sum clearance_{enzymes}} * 100 \tag{4}$$

GC-MS standard urine screening approach (SUSA)

The sample preparation procedure was as published before [15]. Briefly, the urine samples were submitted to acid hydrolysis of phase II conjugates and extracted with a dichloromethane–isopropanol–ethyl acetate mixture (1:1:3 v/v/v) afterwards. After evaporation, the residue was acetylated with an acetic anhydride–pyridine mixture under microwave irradiation, again

evaporated and reconstituted in 100 µL of methanol. The GC and MS conditions for analysis of the extracts were the same as described above for the metabolism studies.

Mass chromatography with the extracted ions at m/z 58, 86, 100, 131, 147, 160, 163, 174, 190, 206, 218, and 220 for acetylated 5-APB, 5-MAPB, and their metabolites was used for toxicological detection. The identity of the peaks in the mass chromatograms was confirmed by computerized comparison of the mass spectra underlying the peaks (after background subtraction) with reference spectra recorded during this study. In addition, the automated mass spectral deconvolution and identification system (AMDIS) (http://chemdata.nist.gov/mass-spc/amdis/) was used for evaluation of the full scan data files acquired by the GC-MS system, as described previously [16].

LC-MS^n standard urine screening approach

A 100-µL aliquot urine was diluted with 500 µL acetonitrile, shaken, centrifuged, evaporated to dryness, and reconstituted in mobile phase A/B (v/v; 50:50) [7]. Analysis was performed using a TF LXQ linear ion trap MS equipped with an HESI II source and coupled to a TF Accela LC system. The LC conditions were as described for LC-HR-MS^n and the MS settings are described elsewhere [7]. Briefly, data-dependent acquisition (DDA) was conducted on precursor ions selected from MS^1: MS^1 was performed in the full scan mode (m/z 100–800). MS^2 and MS^3 were performed in the DDA mode: four DDA MS^2 scan filters were chosen to provide MS^2 on the four most intense signals from MS^1 and additionally, eight MS^3 scan filters were chosen to record MS^3 on the most and second most intense signals from the MS^2.

Plasma samples, sample preparation, and quantification of 5-MAPB and 5-APB

Human blank plasma samples from a local blood bank were used after pH adjustment (pH 7.4 with 10 mM phosphate buffer, dilution factor 5–8 %). Authentic routine heparinized blood plasma samples were submitted to the authors' laboratory by various hospitals for toxicological diagnostics. The samples were centrifuged and the separated plasma was kept frozen (−20 °C) until further processing. Sample preparation consisted of the solid-phase extraction described above and modified according to Peters et al. [17]. MDMA-d$_5$ (50 µg/L final plasma concentration) was used as internal standard and added before extraction. After evaporation to dryness, the residual was derivatized with heptafluorobutyric anhydride under microwave irradiation (450 W, 5 min). After cooling, cyclohexane and sodium phosphate solution was added, mixed, centrifuged, and afterwards the upper layer was transferred to an autosampler vial and 3 µL was injected onto the GC-MS.

Quantification was carried out by comparison of peak area ratios (analyte vs. IS) with calibration curves in which peak area ratios of spiked calibrators were plotted against their concentrations.

Method validation for 5-MAPB quantification

The method was validated as recommended for single case analysis, including selectivity, linearity, accuracy and precision, and limit of quantification [18]. Selectivity was determined by analyzing six blank plasma samples from different sources in selected ion monitoring mode (SIM) mode to check for signals that might interfere with 5-MAPB, 5-APB, or the IS. In addition, two zero samples (blank plasma including IS) were analyzed. The calibration at six different concentrations (1, 5, 10, 50, 100, and 150 μg/L) was performed in duplicate and analyzed as described above. The regression line was calculated using a first-order polynomial weighted $(1/x)$ least-squares model.

Six quality control (QC) samples at low (2 μg/L) and high (120 μg/L) concentrations were analyzed and determined based on daily calibration curves. Accuracy was calculated in terms of bias as the percent deviation of the mean calculated concentration at each concentration from the corresponding theoretical concentration. Precision was calculated as the relative standard deviation (RSD). The limit of quantification (LOQ) of the method was defined as the concentration of the lowest calibrator and was checked for the acceptance criterion of a signal-to-noise (S/N) ratio of >10.

GC-MS apparatus for quantification of plasma concentrations

Analysis was performed with the GC-MS apparatus described above but with the following modifications: column, Optima 5 MS capillary (25 m × 0.2 mm I.D.; Macherey-Nagel, Düren, Germany); column temperature, programmed from 80 to 200 °C at 5 °C/min, 2 min hold, 200–310 °C at 35 °C/min, initial time 2 min, final time 3 min; total time 34 min; carrier gas, helium; flow rate, 0.8 mL/min. The MS conditions were modified as follows: SIM with ions at m/z 131 (quantifier), 158, and 240 for 5-APB and m/z 131, 158, and 254 (quantifier) for 5-MAPB, and m/z 164, 213, and 258 (quantifier) for the internal standard MDMA-d_5.

Results and discussion

GC-MS identification of phase I metabolites

In order to elucidate the metabolite structures, the fragments in the EI spectra of the metabolites were interpreted in correlation to that of the parent compound. The fragmentation patterns of other amphetamines or benzofurans [4, 11] and the general fragmentation rules described by, e.g., Smith and Bush or McLafferty were taken into consideration [19, 20]. Furthermore, the metabolism of other furan or benzofuran containing compounds was considered [21–27]. Figure 1 shows the EI mass spectra, structures, predominant fragmentation patterns, and GC retention indices (RI) of the acetylated parent compounds and their acetylated metabolites (1.1–1.11). These data were also a prerequisite for studying the detectability of the compounds by the GC-MS SUSA.

EI-MS fragmentation of the phase I metabolites

In the following, important fragmentation patterns of the EI mass spectra of acetylated 5-APB and 5-MAPB and their metabolites will be discussed in detail allowing postulation of the structures depicted in Fig. 1 (1–11). The numbers of the corresponding mass spectra are given in brackets. As can be seen, 5-APB and most of its metabolites are also the corresponding N-demethyl metabolites of 5-MAPB. Many spectra show fragment ions either at m/z 86 or 58 and 100 [e.g., Fig. 1 (1, 2, or 5, 7)] resulting from a cleavage between position 1 and 2 in the propylamine side chain. Fragment ion at m/z 86 represents the acetylated ethaniminium ion, specific in this case for primary amines such as 5-APB, its metabolites, and the N-demethyl metabolites of 5-MAPB. Ion at m/z 100 corresponds to the acetylated N-methyl-ethaniminium ion and 58 to the underivatized N-methyl-ethaniminium ion, both specific for 5-MAPB and its non-N-demethylated metabolites. The spectra of acetylated 5-APB (1) and 5-MAPB (2) show two specific fragment ions at m/z 131 and 158, resulting from alpha cleavage or the loss of either acetamide (59 u) or N-methylacetamide (73 u) and representing the benzofuranyl-methylium or the benzofuranyl-propylium ion. Metabolic deamination was found for the investigated compounds as already described for primary amines such as amphetamine or phenethylamines of the 2C series [28, 29]. The hydroxy-deamino-dihydro metabolite (3) shows fragment ions at m/z 147 and 174, each indicating the introduction of one oxygen atom (16 u) to fragment ions at m/z 131 and 158. Fragment ions at m/z 189 and 216 represent either the acetylated hydroxy-benzofuranyl-methylium ion or resulted from the loss of acetic acid (60 u) from the precursor ion (m/z 276). The spectrum of twofold acetylated hydroxy 5-APB or N-demethyl-hydroxy 5-MAPB (4) showed the same fragment ions as the hydroxy-deamino-dihydro metabolites, except of the precursor ion at m/z 275, and a loss of acetamide led to ion m/z 216. For both compounds, ring opened metabolites could be observed as described for other benzofuran containing compounds [21, 22]. Kobayashi et al. studied the mechanism of metabolic cleavage of furan rings with the model compound TA-1801. Using deuterium-labeled compounds, they could show that the C–O bond of the furan ring was cleaved
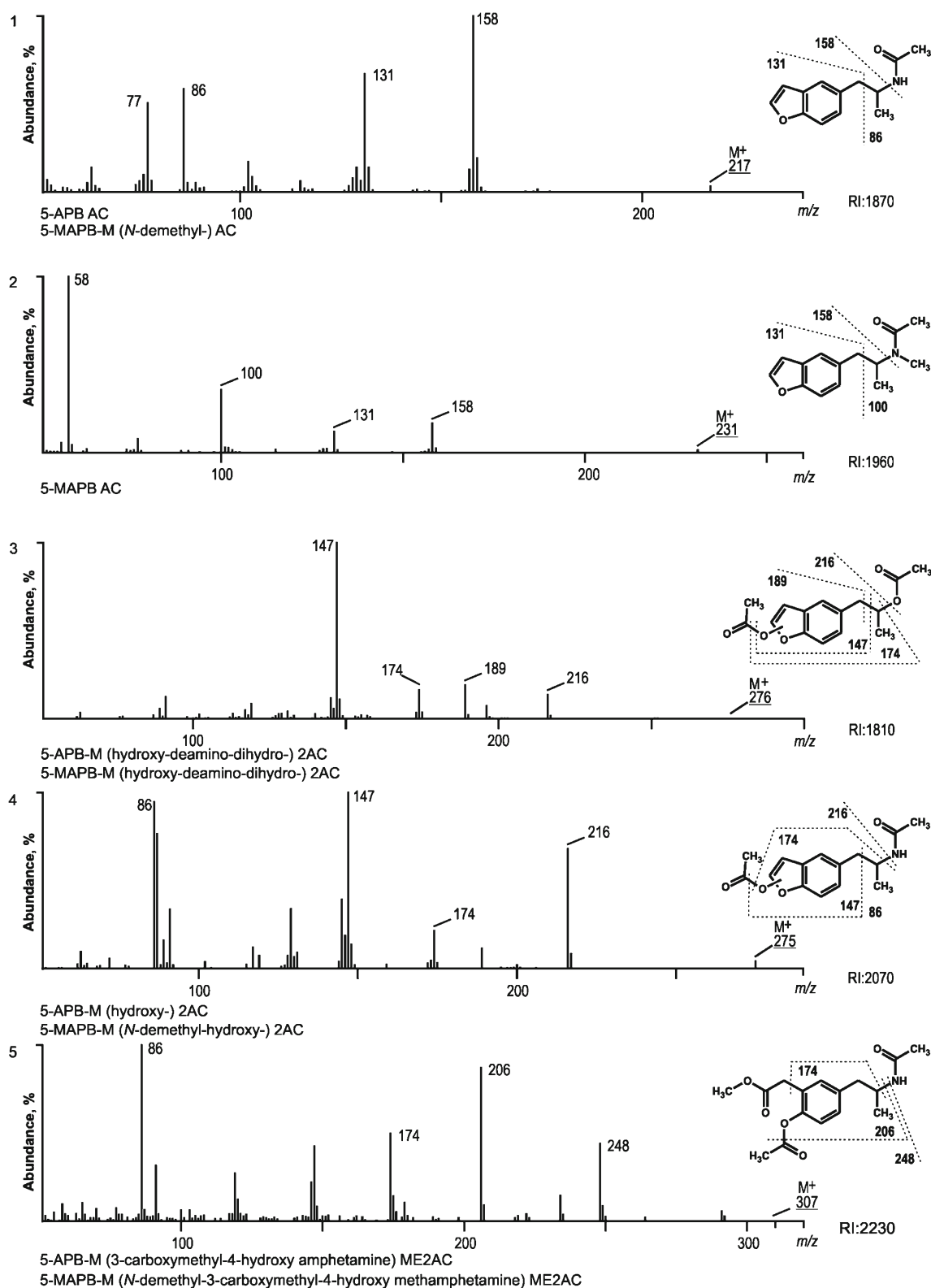
Fig. 1 EI mass spectra, gas chromatographic retention indices (RI), proposed structures, and predominant fragmentation patterns of acetylated 5-APB (*1.1*), 5-MAPB (*1.2*), and their metabolites (*1.3–1.11*) arranged according to their RI

by CYPs forming unsaturated aldehydes. They also incubated the synthesized unsaturated aldehyde with rat liver microsomes to show that this was the intermediate for the resulting carboxy or alcoholic metabolite. Catalyzing
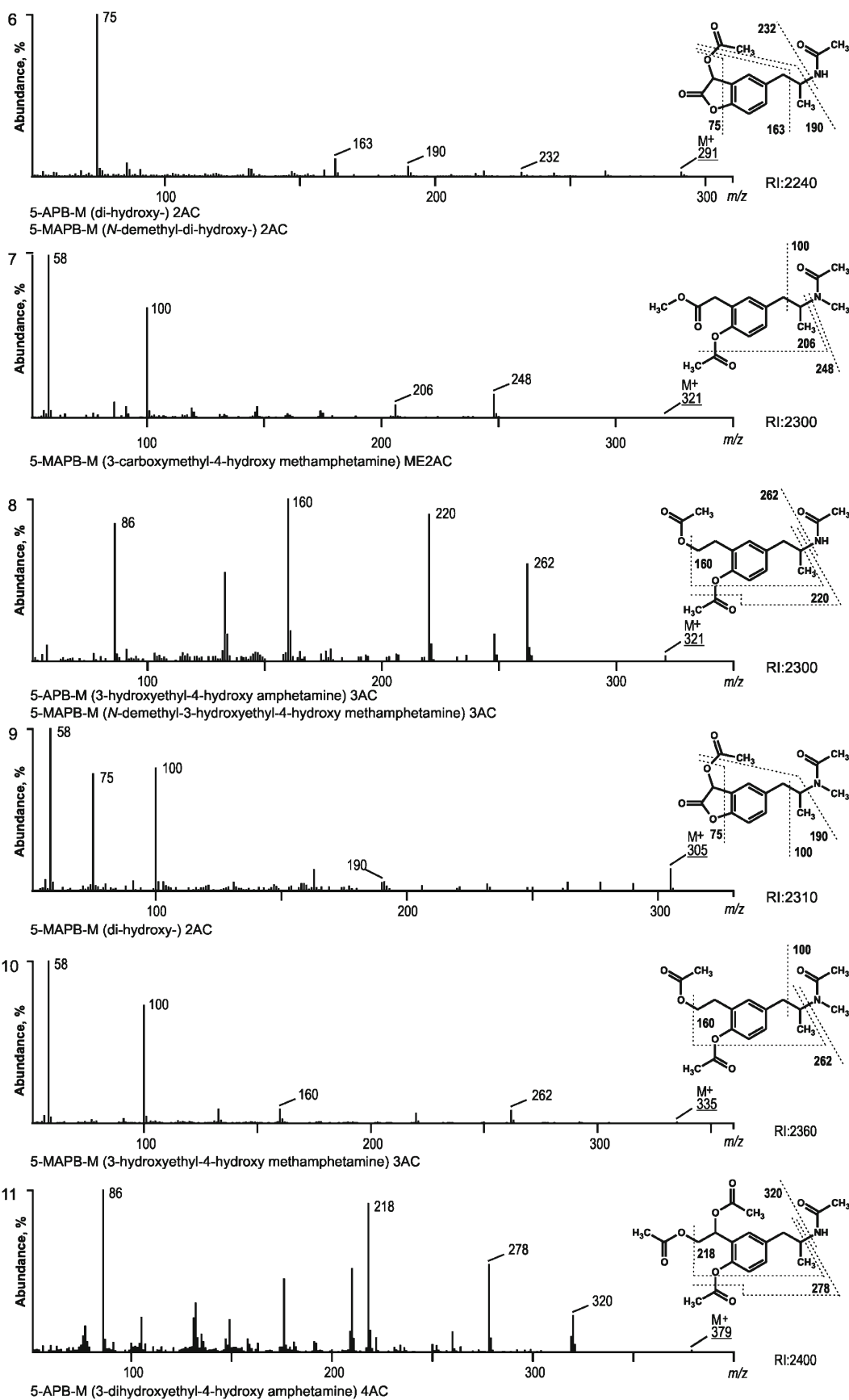
5-APB-M (di-hydroxy-) 2AC
5-MAPB-M (*N*-demethyl-di-hydroxy-) 2AC

5-MAPB-M (3-carboxymethyl-4-hydroxy methamphetamine) ME2AC

5-APB-M (3-hydroxyethyl-4-hydroxy amphetamine) 3AC
5-MAPB-M (*N*-demethyl-3-hydroxyethyl-4-hydroxy methamphetamine) 3AC

5-MAPB-M (di-hydroxy-) 2AC

5-MAPB-M (3-hydroxyethyl-4-hydroxy methamphetamine) 3AC

5-APB-M (3-dihydroxyethyl-4-hydroxy amphetamine) 4AC

Fig. 1 (continued)

enzymes for the following steps should be aldehyde oxidase and alcohol dehydrogenase. This is consistent with the mechanism described by Connelly et al. [21]. The spectra of the methylesters of twofold acetylated 3-carboxymethyl-4-hydroxy amphetamine or N-demethyl-3-carboxymethyl-4-hydroxy methamphetamine (5) and 3-carboxymethyl-4-hydroxy methamphetamine (7) show fragment ions at m/z 206 and 248, resulting from cleavage between position 1 and 2 and subsequent loss of the acetyl group. The fragment ions in the spectra of twofold acetylated di-hydroxy 5-APB/N-demethyl-di-hydroxy 5-MAPB (6) and di-hydroxy 5-MAPB (9) were at m/z 75, 163, and 190. The ions at m/z 163 and 190 resulted from the introduction of a second oxygen atom to the benzofuran ring whereas ion at m/z 75 should result from the cleavage of the benzofuran ring to a tri-hydroxy-ethenylium ion which may be due to increased mesomeric effects. Other metabolites with benzofuran cleavage were threefold acetylated 3-hydroxyethyl-4-hydroxy amphetamine or N-demethyl-3-hydroxyethyl-4-hydroxy methamphetamine (8) and 3-hydroxyethyl-4-hydroxy methamphetamine (10). Predominant fragment ions were at m/z 160, 220, and 262. The loss of either acetamide or N-methyl-acetamide from the precursor ion resulted in ion at m/z 262, and the subsequent loss of one acetyl group and acetic acid then led to fragment ions at m/z 220 or 160, respectively. Abundant fragment ions in the spectrum of peracetylated 3-dihydroxyethyl-4-hydroxy amphetamine (11) were at m/z 320, 278, and 218, resulting from subsequent loss of acetamide, acetyl group, and acetic acid from the side chain.

LC-HR-MS^n confirmation of phase I metabolites

Using LC-HR-MS^n, all metabolites identified by GC-MS could be confirmed with the exception of hydroxy-deamino-dihydro 5-APB/hydroxy-deamino-dihydro 5-MAPB (3), di-hydroxy 5-APB (6), N-demethyl-di-hydroxy 5-MAPB (6), and di-hydroxy 5-MAPB (9) probably because of poor ionization or instability in the ion source. On the other hand, four additional metabolites could be detected, namely hydroxy-dihydro 5-APB/N-demethyl-hydroxy-dihydro 5-MAPB (12), hydroxy 5-MAPB (13), hydroxy-dihydro 5-MAPB (14), and 3-dihydroxyethyl-4-hydroxy methamphetamine (15). In Table 1, all identified acetylated phase I metabolites of 5-APB and 5-MAPB are listed together with the accurate and the calculated exact masses, the corresponding two main fragment ions in MS^2 and the two most abundant fragment ion in the corresponding MS^3 spectra, the corresponding elemental compositions, the deviations of the measured accurate masses from the calculated masses, given as errors in parts per million, and the retention times. All measured masses were within 5 ppm deviation.

HESI-HR-MS^n fragmentation of the phase I metabolites

In the following, the fragmentation of 5-APB, 5-MAPB, and their metabolites will be explained in detail according to the fragments given in Table 1. The MS^2 spectrum of underivatized 5-APB (1a; protonated molecular mass, PM, at m/z 176.1065) showed two fragments, the benzofuranyl-methylium ion at m/z 131.0492 resulting from an alpha cleavage and the fragment ion at m/z 117.0699 resulting from loss of oxygen followed by ring closure. Since underivatized 5-APB formed no MS^3 spectra, all HR spectra were recorded in urine extracts after acetylation as approved in former studies [9]. This resulted in formation of more specific spectra due to more fragment ions. The MS^2 spectrum of acetylated 5-APB (1b; PM at m/z 218.1166) showed the most abundant fragment ions at m/z 159.0805 and 176.1071. Loss of the acetyl group resulted in the underivatized parent compound (m/z 176) and following loss of ammonia resulted in the benzofuranyl-propylium ion at m/z 159. Fragments in the MS^3 spectra were at m/z 131.0492, 117.0699, and 159.0797. Although underivatized 5-MAPB (2a, PM at m/z 190.1218) formed more fragments, the acetylated extracts were also used. Acetylated 5-MAPB (2b; PM at m/z 232.1322) showed fragment ions at m/z 190.1229 (42.0105 u for loss of the acetyl group) and 159.0806 for the benzofuranyl-propylium ion. The MS^2 of twofold acetylated hydroxy 5-APB (4; PM at m/z 276.1227) and of twofold acetylated hydroxy 5-MAPB (13; PM at m/z 290.1382) showed fragment ions at m/z 217.0859 after loss of acetamide (59.0371 u) and N-methyl-acetamide (73.0527 u), respectively. An alternative loss of only the acetyl group resulted in fragment ions at m/z 234.1125 or 248.1281. The most abundant fragment ion in MS^3 was at m/z 175.0752, resulting from the loss of the second acetyl group from ion at m/z 234 and 248, respectively, and representing the hydroxy-benzofuranyl-propylium ion (shift of 16 u from m/z 159). Fragment ion at m/z 189.0544, the acetoxy-benzofuranyl-methylium ion, resulted from alpha cleavage. In addition, fragment ion at m/z 192.1018, representing underivatized hydroxy 5-APB, could be detected in the MS^3 spectrum of fragment ion at m/z 234. The MS^2 spectrum of the methylester of twofold acetylated 3-carboxymethyl-4-hydroxy amphetamine (5; PM at m/z 308.1481) showed fragment ions at m/z 266.1385 (loss of one acetyl group) and 234.1125 (loss of the methyl group from the ester and a subsequent loss of water from the carboxy group). In the MS^3 spectra, the fragment ion at m/z 207.1015 resulted from the loss of acetamide from fragment ion at m/z 266.1385, whereas fragment ion at m/z 206.1175 resulted from cleavage of one acetyl group and subsequent loss of water. Fragment ions at m/z 192.1018 and 175.0752 resulted from loss of another acetyl group followed by the loss of ammonia. The spectrum of 3-carboxymethyl-4-hydroxy methamphetamine (7; PM at m/z 322.1646) showed fragment ions at m/z 280.1542 and 248.1281, resulting from

Table 1 List of 5-APB, 5-MAPB, and all acetylated phase I metabolites together with the measured accurate and the calculated exact masses of their PM recorded in MS^1, the corresponding main fragment ions in MS^2 and MS^3, the corresponding elemental compositions, the deviations of the measured accurate masses from the calculated masses, given as errors in parts per million, and the retention times

Number	Metabolites and characteristic ions Measured accurate masses (u)		Calculated exact masses (u)	Elemental composition	Error (ppm)	RT (min)
1a	5-APB					5.4
	5-MAPB-M (*N*-demethyl-)					
	MS^1	PM at *m/z* 176.1065	176.1069	C11H14NO	−2.57	
	MS^2	Fragment ion at *m/z* 131.0492	131.0491	C9H7O	0.26	
		Fragment ion at *m/z* 117.0699	117.0698	C9H9	0.20	
	MS^3	n.d.				
1b	5-APB AC					10.9
	5-MAPB-M (*N*-demethyl-) AC					
	MS^1	PM at *m/z* 218.1166	218.1175	C13H16NO2	−4.42	
	MS^2	Fragment ion at *m/z* 159.0805	159.0804	C11H11O	0.18	
		Fragment ion at *m/z* 176.1071	176.1069	C11H14NO	0.63	
	MS^3	Fragment ion at *m/z* 131.0492	131.0491	C9H7O	0.40	
		Fragment ion at *m/z* 117.0699	117.0698	C9H9	0.59	
		Fragment ion at *m/z* 131.0491	131.0491	C9H7O	0.05	
		Fragment ion at *m/z* 159.0797	159.0804	C11H11O	−4.66	
2a	5-MAPB					6.3
	MS^1	PM at *m/z* 190.1218	190.1226	C12H16NO	−4.21	
	MS^2	Fragment ion at *m/z* 159.0806	159.0804	C11H11O	0.87	
		Fragment ion at *m/z* 131.0493	131.0491	C9H7O	1.28	
	MS^3	Fragment ion at *m/z* 131.0491	131.0491	C9H7O	−0.06	
		Fragment ion at *m/z* 117.0699	117.0698	C9H9	0.01	
2b	5-MAPB AC					13.1
	MS^1	PM at *m/z* 232.1322	232.1332	C14H18NO2	−4.33	
	MS^2	Fragment ion at *m/z* 159.0806	159.0804	C11H11O	0.80	
		Fragment ion at *m/z* 190.1229	190.1226	C12H16NO	1.47	
	MS^3	Fragment ion at *m/z* 131.0491	131.0491	C9H7O	0.05	
		Fragment ion at *m/z* 117.0699	117.0698	C9H9	0.01	
		Fragment ion at *m/z* 159.0797	159.0804	C11H11O	−0.65	
4	5-APB-M (hydroxy-) 2AC					10.1
	5-MAPB-M (*N*-demethyl-hydroxy-) 2AC					
	MS^1	PM at *m/z* 276.1227	276.1230	C15H18NO4	−1.28	
	MS^2	Fragment ion at *m/z* 217.0859	217.0864	C13H13O3	0.12	
		Fragment ion at *m/z* 234.1125	234.1124	C13H16NO3	0.08	
	MS^3	Fragment ion at *m/z* 175.0752	175.0753	C11H11O2	−0.91	
		Fragment ion at *m/z* 189.0544	189.0551	C11H9O3	−1.09	
		Fragment ion at *m/z* 175.0752	175.0753	C11H11O2	−0.74	
		Fragment ion at *m/z* 192.1018	192.1019	C11H14NO2	−0.59	
5	5-APB-M (3-carboxymethyl-4-hydroxy amphetamine) ME2AC					9.7
	5-MAPB-M (*N*-demethyl-3-carboxymethyl-4-hydroxy methamphetamine) ME2AC					
	MS^1	PM at *m/z* 308.1481	308.1492	C16H22NO5	−3.82	
	MS^2	Fragment ion at *m/z* 266.1385	266.1386	C14H20NO4	−0.69	
		Fragment ion at *m/z* 234.1125	234.1124	C13H16NO3	0.07	
	MS^3	Fragment ion at *m/z* 206.1175	206.1175	C12H16NO2	−0.45	
		Fragment ion at *m/z* 207.1015	207.1021	C12H15O3	−0.34	
		Fragment ion at *m/z* 175.0754	175.0753	C11H11O2	0.38	
		Fragment ion at *m/z* 192.1018	192.1019	C11H14NO2	0.59	

Table 1 (continued)

Number	Metabolites and characteristic ions Measured accurate masses (u)		Calculated exact masses (u)	Elemental composition	Error (ppm)	RT (min)
7	5-MAPB-M (3-carboxymethyl-4-hydroxy methamphetamine) ME2AC					11.3
	MS[1]	PM at *m/z* 322.1646	322.1648	C17H24NO5	−2.69	
	MS[2]	Fragment ion at *m/z* 280.1542	280.1543	C15H22NO4	−0.46	
		Fragment ion at *m/z* 248.1281	248.1281	C14H18NO3	−0.02	
	MS[3]	Fragment ion at *m/z* 207.1017	207.1015	C11H13O2	0.47	
		Fragment ion at *m/z* 220.1333	220.1332	C13H18NO2	0.43	
8	5-APB-M (3-hydroxyethyl-4-hydroxy amphetamine) 3AC 5-MAPB-M (*N*-demethyl-3-hydroxyethyl-4-hydroxy methamphetamine) 3AC					11.3
	MS[1]	PM at *m/z* 322.1636	322.1648	C17H24NO5	−4.12	
	MS[2]	Fragment ion at *m/z* 280.1543	280.1543	C15H22NO4	−0.23	
		Fragment ion at *m/z* 262.1438	262.1437	C15H20NO3	0.23	
	MS[3]	Fragment ion at *m/z* 220.1333	220.1332	C13H18NO2	0.25	
		Fragment ion at *m/z* 238.1438	238.1437	C13H20NO3	−0.01	
		Fragment ion at *m/z* 220.1333	220.1332	C13H18NO2	0.57	
		Fragment ion at *m/z* 161.0962	161.0960	C11H13O	0.43	
10	5-MAPB-M (3-hydroxyethyl-4-hydroxy methamphetamine) 3AC					12.9
	MS[1]	PM at *m/z* 336.1792	336.1805	C18H26NO5	−4.36	
	MS[2]	Fragment ion at *m/z* 294.1701	294.1699	C16H24NO4	0.30	
		Fragment ion at *m/z* 276.1596	276.1594	C16H22NO3	0.67	
	MS[3]	Fragment ion at *m/z* 252.1592	252.1594	C14H22NO3	−0.77	
		Fragment ion at *m/z* 234.1487	234.1488	C14H20NO2	−0.67	
		Fragment ion at *m/z* 234.1487	234.1488	C14H20NO2	−0.54	
		Fragment ion at *m/z* 161.0960	161.0960	C11H13O	−0.61	
11	5-APB-M (3-dihydroxyethyl-4-hydroxy amphetamine) 2AC					11.7
	MS[1]	PM at *m/z* 296.1487	296.1492	C15H22NO5	−1.91	
	MS[2]	Fragment ion at *m/z* 219.1012	219.1015	C13H15O3	−1.57	
		Fragment ion at *m/z* 237.1118	237.1121	C13H17O4	−1.41	
	MS[3]	Fragment ion at *m/z* 177.0908	177.0910	C11H13O2	−1.04	
		Fragment ion at *m/z* 159.0803	159.0804	C11H11O	−1.03	
12	5-APB-M (hydroxy-dihydro-) 2AC 5-MAPB-M (*N*-demethyl-hydroxy-dihydro-) 2AC					11.5
	MS[1]	PM at *m/z* 278.1379	278.1386	C15H20NO4	−2.67	
	MS[2]	Fragment ion at *m/z* 236.1282	236.1281	C13H18NO3	0.34	
		Fragment ion at *m/z* 218.1177	218.1175	C13H16NO2	0.66	
	MS[3]	Fragment ion at *m/z* 177.0910	177.0910	C11H13O2	0.07	
		Fragment ion at *m/z* 194.1176	194.1175	C11H16NO2	0.38	
		Fragment ion at *m/z* 159.0804	159.0804	C11H11O	0.01	
		Fragment ion at *m/z* 176.1070	176.1069	C11H14NO	0.19	
13	5-MAPB-M (hydroxy-) 2AC isomer 2					12.1
	MS[1]	PM at *m/z* 290.1382	290.1386	C16H20NO4	1.00	
	MS[2]	Fragment ion at *m/z* 217.0861	217.0864	C13H13O3	1.07	
		Fragment ion at *m/z* 248.1282	248.1281	C14H18NO3	0.63	
	MS[3]	Fragment ion at *m/z* 175.0756	175.0753	C11H11O2	0.46	
		Fragment ion at *m/z* 217.0862	217.0859	C13H13O3	0.49	
		Fragment ion at *m/z* 175.0754	175.0753	C11H11O2	0.38	
		Fragment ion at *m/z* 189.0547	189.0546	C11H9O3	0.27	

Table 1 (continued)

Number	Metabolites and characteristic ions Measured accurate masses (u)		Calculated exact masses (u)	Elemental composition	Error (ppm)	RT (min)
14	5-MAPB-M (hydroxy-dihydro-) 2AC					12.4
	MS^1	PM at m/z 292.1539	290.1543	C16H22NO4	−1.59	
	MS^2	Fragment ion at m/z 250.1439	250.1437	C14H20NO3	0.64	
		Fragment ion at m/z 232.1335	232.1332	C14H18NO2	1.09	
	MS^3	Fragment ion at m/z 177.0910	177.0910	C11H13O2	0.24	
		Fragment ion at m/z 208.1333	208.1332	C12H18NO2	0.53	
		Fragment ion at m/z 159.0804	159.0804	C11H11O	0.20	
		Fragment ion at m/z 190.1227	190.1226	C12H16NO	0.13	
15	5-MAPB-M (3-dihydroxyethyl-4-hydroxy methamphetamine) 4AC					12.8
	MS^1	PM at m/z 394.1858	394.1860	C20H28NO7	−3.62	
	MS^2	Fragment ion at m/z 334.1643	334.1648	C18H24NO5	−1.75	
		Fragment ion at m/z 352.1749	352.1754	C18H26NO6	−1.68	
	MS^3	Fragment ion at m/z 292.1542	292.1543	C16H22NO4	−0.44	

the same loss of one acetyl group and the subsequent loss of the methyl group from the ester and water. In the MS^3 of 280.1542, fragment ions were observed at m/z 207.1017, resulting from the loss of N-methyl-acetamide (73 u), and at m/z 220.1333, resulting from cleavage of one acetyl group and a subsequent loss of water. The MS^2 spectrum of threefold acetylated 3-hydroxyethyl-4-hydroxy amphetamine (8; PM at m/z 322.1636) showed fragment ions at m/z 280.1543 resulting from loss of one acetyl group and fragment ion at m/z 262.1438 indicating the hydroxy group at the alkyl chain because of the loss of water (18.0105 u) from m/z 280.1543. The most abundant fragment ions in the MS^3 spectra were formed by loss of an acetyl group from fragment at m/z 262 or loss of one acetyl group followed by loss of water from fragment at m/z 280.1543 resulting in fragment ions at m/z 238.1438 and 220.1333. Fragment ion at m/z 161.0962 represents the 4-hydroxy-3-vinylphenyl-propylium ion resulting from loss of acetamide from fragment at m/z 220.1333. The MS^2 spectrum of threefold acetylated 3-hydroxyethyl-4-hydroxy methamphetamine (10; PM at m/z 336.1792) showed fragment ions at m/z 294.1701, resulting from loss of one acetyl group, and at m/z 276.1596 from loss of water. The corresponding MS^3 spectra showed either fragment ions at m/z 252.1592, after the loss of another acetyl group and after water loss at m/z 234.1487. Twofold acetylated 3-dihydroxyethyl-4-hydroxy amphetamine (11; PM at m/z 296.1487) showed in the MS^2 spectrum as most abundant fragment ions those at m/z 237.1118 and 219.1012, resulting from loss of acetamide and water. The MS^3 spectrum of fragment ion at m/z 219.1012 showed the ions at m/z 177.0908 and 159.0803 resulting from the loss of one acetyl group followed by the loss of water. The most abundant fragments in the MS^2 spectrum of hydroxy-dihydro 5-APB (12; PM at m/z 278.1379) were those at m/z 236.1282 resulting from

the loss of one acetyl group and at m/z 218.1177 after a following water loss. Fragment ions at m/z 194.1176 and 177.0910 were present in the MS^3 spectrum of fragment ion at m/z 236 representing the underivatized hydroxy-dihydro 5-APB and, after loss of ammonia (17.0265 u), the corresponding hydroxy-dihydro-benzofuranyl-propylium ion. The MS^3 spectrum of fragment ion at m/z 218.1177 showed the most abundant ions at m/z 159.0804 and 176.1070 being the same as for acetylated 5-APB. These fragments indicated that the described metabolite is the hydroxy-dihydro 5-APB as a loss of acetic acid (60 u) from the benzofuran part forms acetylated 5-APB. The MS^2 spectrum of twofold acetylated hydroxy-dihydro 5-MAPB (14; PM at m/z 292.1539) showed the fragment ion at m/z 250.1439 resulting from loss of one acetyl group and at m/z 232.1335 after a subsequent water loss. The MS^3 spectra showed either the same fragments as the corresponding N-demethyl metabolite (at m/z 177.0910 and 159.0804) or fragments at m/z 208.1333 and 190.1227, representing unacetylated hydroxy-dihydro 5-MAPB or after loss of water 5-MAPB. Fragment ions present in the MS^2 spectrum of fourfold acetylated 3-dihydroxyethyl-4-hydroxy methamphetamine (15; PM at m/z 394.1858) were at m/z 334.1643 and 352.1749, resulting from the stepwise loss of one acetyl group and water. Another loss of one acetyl group to fragment ion at m/z 292.1542 was observed in the corresponding MS^3 of m/z 334.1643.

HESI-HR-MS^n fragmentation and identification of the phase II metabolites

Glucuronides and/or sulfates were identified by two different methods: either by searching for a specific neutral loss of 176.0320 u for glucuronides and/or 79.9568 u for sulfates,

or by using the data-dependent scan mode on the expected precursor ions. The detected glucuronides were, if possible, identified by comparing their MS^2 and MS^3 with the MS^1 and MS^2 spectra of the corresponding phase I metabolites. In Table 2, all identified phase II metabolites are listed together with the accurate and the calculated exact masses, the corresponding two main fragment ions in MS^2 and the two most abundant fragment ion in the corresponding MS^3 spectra (if available), the corresponding elemental compositions, the deviations of the measured accurate masses from the calculated masses, given as errors in parts per million, and the retention times. Again, all measured masses were within 5 ppm deviation.

Altogether, no sulfates and only few glucuronides could be observed. For 5-APB, the following glucuronides could be detected: 3-carboxymethyl-4-hydroxy amphetamine glucuronide (5G) and 3-hydroxyethyl-4-hydroxy amphetamine glucuronide (8G). For 5-MAPB, N-demethyl-3-carboxymethyl-4-hydroxy methamphetamine glucuronide (5G), 3-carboxymethyl-4-hydroxy methamphetamine glucuronide (7G), N-demethyl-3-hydroxyethyl-4-hydroxy methamphetamine glucuronide (8G), and two isomers of the 3-hydroxyethyl-4-hydroxy methamphetamine glucuronide (10.1G/10.2G) could be detected.

In summary, all MS^2 spectra showed after the specific neutral loss of 176 u for glucuronides the corresponding phase I metabolite. For example, the 3-carboxymethyl-4-hydroxy amphetamine glucuronide/N-demethyl 3-carboxymethyl-4-hydroxy methamphetamine glucuronide (5G; PM at m/z 386.1429) showed in MS^2 most abundant fragment ions at m/z 210.1120 and m/z 193.0855, representing the phase I

Table 2 List of 5-APB and 5-MAPB phase II metabolites together with the measured accurate and the calculated exact masses of their PM recorded in MS^1, the corresponding main fragment ions in MS^2 and MS^3, if available, the corresponding elemental compositions, the deviations of the measured accurate masses from the calculated masses, given as errors in parts per million, and the retention times

Number	Metabolites and characteristic ions Measured accurate masses (u)	Calculated exact masses (u)	Elemental composition	Error (ppm)	RT (min)
5G	5-APB-M (3-carboxymethyl-4-hydroxy amphetamine glucuronide) 5-MAPB-M (N-demethyl-3-carboxymethyl-4-hydroxy methamphetamine glucuronide)				3.3
	MS^1 PM at m/z 386.1429	386.1445	C17H24NO9	−4.26	
	MS^2 Fragment ion at m/z 210.1120	210.1120	C11H16NO3	−2.31	
	Fragment ion at m/z 193.0855	193.0855	C11H13O3	−2.30	
	MS^3 Fragment ion at m/z 175.0749	175.0749	C11H11O2	−2.66	
	Fragment ion at m/z 147.0437	147.0440	C9H7O2	−2.72	
	Fragment ion at m/z 147.0800	147.0804	C10H11O	−2.78	
7G	5-MAPB-M (3-carboxymethyl-4-hydroxy methamphetamine glucuronide)				2.6
	MS^1 PM at m/z 400.1583	400.1602	C18H26NO9	−4.69	
	MS^2 Fragment ion at m/z 224.1276	224.1281	C12H18NO3	−2.41	
	Fragment ion at m/z 193.0855	193.0855	C11H13O3	−2.04	
	MS^3 n.d.				
8G	5-APB-M (3-hydroxyethyl-4-hydroxy amphetamine glucuronide) 5-MAPB-M (N-demethyl-3-hydroxyethyl-4-hydroxy methamphetamine glucuronide)				2.6
	MS^1 PM at m/z 372.1636	372.1652	C17H26NO8	−4.44	
	MS^2 Fragment ion at m/z 179.1062	179.1066	C11H15O2	−2.51	
	Fragment ion at m/z 196.1327	196.1332	C11H18NO2	−2.32	
	MS^3 n.d.				
10.1G	5-MAPB-M (3-hydroxyethyl-4-hydroxy methamphetamine glucuronide)				1.7
	MS^1 PM at m/z 386.1787	386.1809	C18H28NO8	−4.90	
	MS^2 Fragment ion at m/z 210.1483	210.1488	C12H20NO2	−2.85	
	Fragment ion at m/z 179.1061	179.1066	C11H15O2	−2.88	
	MS^3 n.d.				
10.2G	5-MAPB-M (3-hydroxyethyl-4-hydroxy methamphetamine glucuronide)				2.6
	MS^1 PM at m/z 386.1790	386.1809	C18H28NO8	−4.94	
	MS^2 Fragment ion at m/z 210.1483	210.1488	C12H20NO2	−2.27	
	Fragment ion at m/z 179.1061	179.1066	C11H15O2	−2.45	
	MS^3 n.d.				

metabolite and after loss of ammonia the 3-carboxymethyl-4-hydroxyphenyl-propylium ion. For the MS^3 spectra, fragment ion at m/z 175.0749 was observed resulting from loss of water from fragment at m/z 193.0855 and either by additional loss of ethylene (28.0313 u) to fragment ion at m/z 147.0437 or carbon monoxide (27.9943 u) to fragment ion at m/z 147.0800. The MS^2 spectrum of 3-hydroxyethyl-4-hydroxy amphetamine/N-demethyl 3-hydroxyethyl-4-hydroxy methamphetamine glucuronide (8G; PM at m/z 372.1636) showed fragment ion at m/z 196.1327 representing the phase I metabolite and fragment ion at m/z 179.1062, resulting from a following loss of ammonia (17 u) and representing the 3-hydroxyethyl-4-hydroxy-phenyl-propylium ion. The MS^2 of 3-carboxymethyl-4-hydroxy methamphetamine (7G; PM at m/z 400.1583) showed fragment ions at m/z 224.1276, after loss of the conjugate, and at m/z 193.0855, after additional loss of methanamine. 3-Hydroxyethyl-4-hydroxy methamphetamine (10.1G/10.2G; PM at m/z 386.1787) showed most abundant fragment ions in MS^2 at m/z 210.1483 representing the corresponding phase I metabolite and at m/z 179.1061 resulting from the loss of methanamine. No MS^3 spectra could be recorded for these metabolites most probably due to low concentrations.

Proposed metabolic pathways

Figure 2 summarizes the main metabolic pathways for 5-APB and 5-MAPB proposed according to the identified metabolites. In accordance to metabolic studies on furan and benzofuran [21, 22, 26], hydroxylation of 5-APB (1) at the furan ring (4) was the initial step. The following ring cleavage and reduction of the resulting unsaturated aldehyde lead to the corresponding aldehyde, which was either oxidized to the corresponding carboxylic acid (5) or reduced to the alcohol (8). The alcohol was further hydroxylated (11) and both carboxylic acid and alcohol were glucuronidated (5G/8G). Further hydroxylation of the hydroxy metabolite could be deduced (6), as well as hydrogenation (12) and deamination followed by reduction (3). For 5-MAPB (2), the predominant step was N-demethylation to 5-APB (1), which underwent the same pathways as described for 5-APB. 5-MAPB itself also underwent most of the described pathways, namely benzofuran hydroxylation (13) followed by enzymatic ring cleavage to either an alcohol (10) by reduction or carboxylic acid (7) by oxidation of the intermediate aldehyde. The alcohol was further hydroxylated (15) and both carboxylic acid and alcohol were glucuronidated (7G, 10.1G/10.2G).
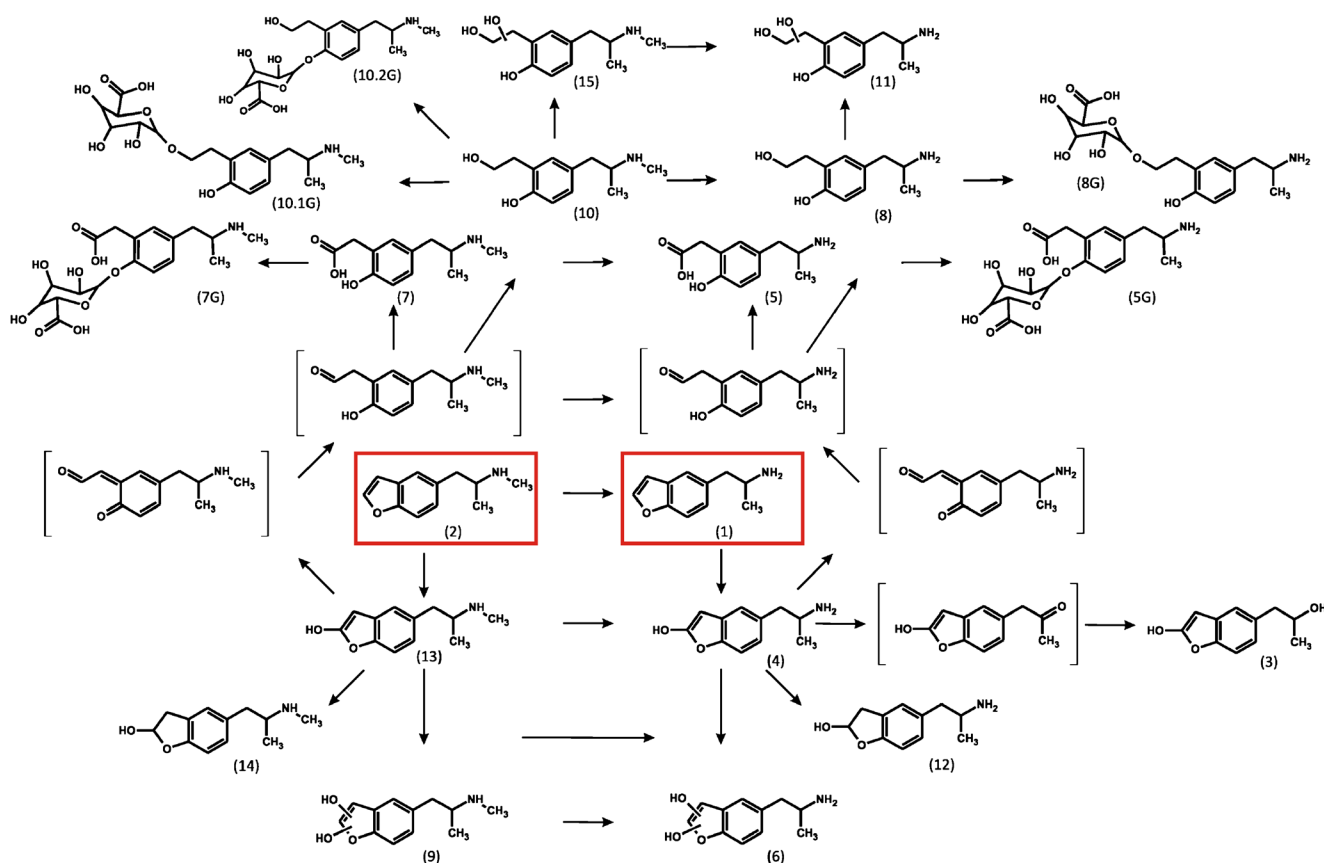
Fig. 2 Proposed metabolic pathways for 5-APB and 5-MAPB in rat

Further pathways were hydroxylation (9) or hydrogenation (14) of the hydroxy metabolite. In summary, *N*-demethylation was the most dominant step due to the corresponding relative GC-MS and LC-MS peak areas for 5-MAPB. Another important step for both compounds, and the most important one for 5-APB, was the enzymatic cleavage of the benzofuran ring leading afterwards to the corresponding carboxy or hydroxy metabolite by oxidation or reduction.

In the human urine samples, after ingestion of unknown doses of 5-MAPB, the following metabolites could be detected after the same sample preparation as described above: *N*-demethyl, hydroxy 5-MAPB, 3-hydroxyethyl-4-hydroxy methamphetamine, and 3-carboxymethyl-4-hydroxy methamphetamine. In the urine of the patient with the highest plasma concentration, *N*-demethyl-3-carboxymethyl-4-hydroxy methamphetamine and *N*-demethyl-3-hydroxyethyl-4-hydroxy methamphetamine 5-MAPB could also be detected.

### HLM incubations and initial CYP activity screening

For comparison whether the rat metabolites can also be formed by humans, the drugs were incubated with HLM. Only a few metabolites in small amounts could be detected in the HLM incubations. For 5-APB, hydroxy 5-APB (4), hydroxy-dihydro 5-APB (12), and as most abundant metabolite, 3-carboxymethyl-4-hydroxy amphetamine (5), were detectable. For 5-MAPB, hydroxy 5-MAPB (13), hydroxy-dihydro 5-MAPB (14), 3-carboxymethyl-4-hydroxy methamphetamine

(7), and most abundantly *N*-demethyl 5-MAPB (1) could be found. This was in accordance to the low-dose rat urine results.

The evaluation of the initial CYP activity screening [9] for the 5-APB metabolism was not possible because of the very low metabolite formation rate. For 5-MAPB, only the *N*-demethylation could be monitored. The enzymes involved in this step were CYP1A2, CYP2B6, CYP2C19, and CYP2D6. The multiple-step reactions, e.g., the ring cleaved metabolites, cannot be formed with recombinant isoenzymes. Other reasons could be low formation rates or inhibition of the enzymes by the corresponding compounds.

Kinetic studies

For *N*-demethylation of 5-MAPB, the kinetic profiles of CYP2D6, CYP2B6, and HLM fit best into Michaelis–Menten kinetics as shown in Fig. 3. The kinetic profiles for CYP1A2 and CYP2C19 indicated substrate inhibition, most likely due to high substrate concentrations needed for enzyme saturation. For these isoenzymes, K_m and V_{max} values could only be estimated by exclusion of the high concentrations. The K_m and V_{max} values are given in Fig. 3. The net clearances for particular P450s were calculated at two different concentrations (10 and 50 μmol/L) [30] and were as follows: 6/8, 39/46, 20/12, and 35/34 % for CYP1A2, CYP2B6, CYP2C19, and CYP2D6, respectively. In conclusion, the net clearance data indicated that CYP2B6 was responsible for the main part of the total 5-MAPB CYP-dependent clearance. This is in accordance with previously published data on the *N*-demethylation
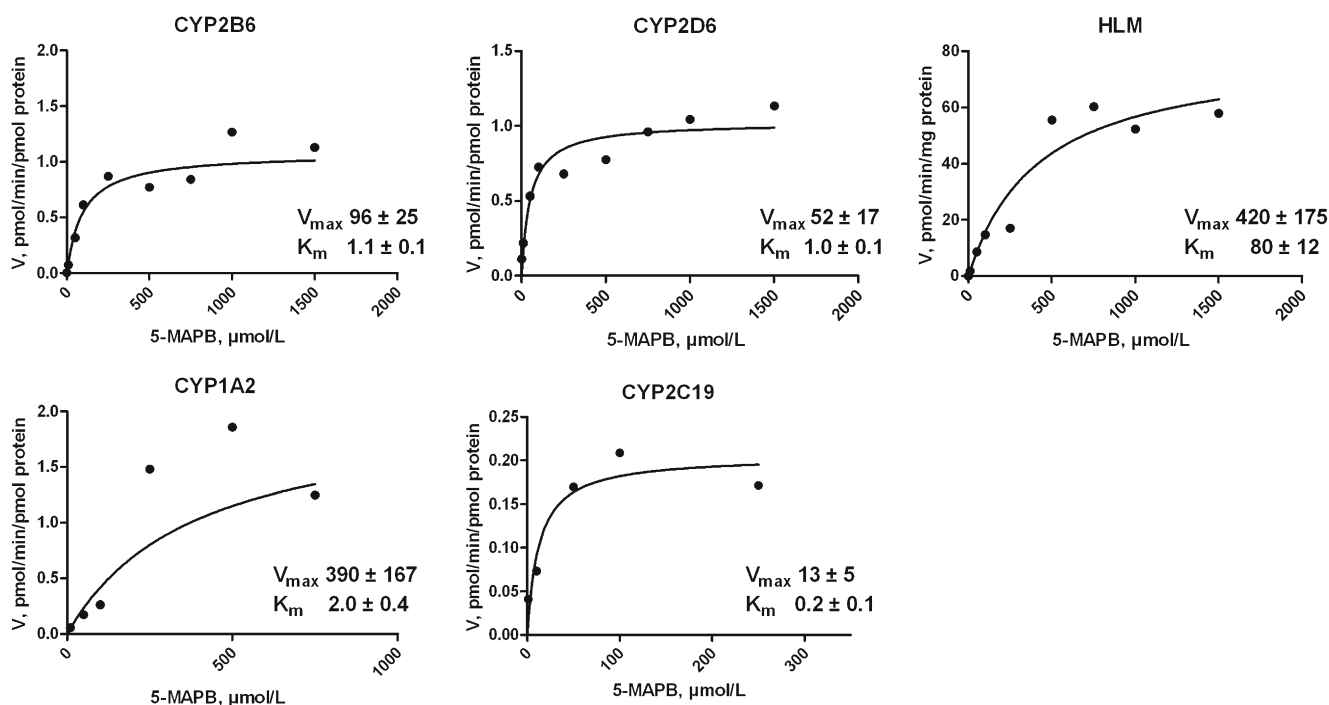
Fig. 3 Enzyme kinetic plots for 5-MAPB *N*-demethylation catalyzed by the given CYP isoenzymes with the corresponding V_{max} and K_m values. Data points represent means of duplicate measurements
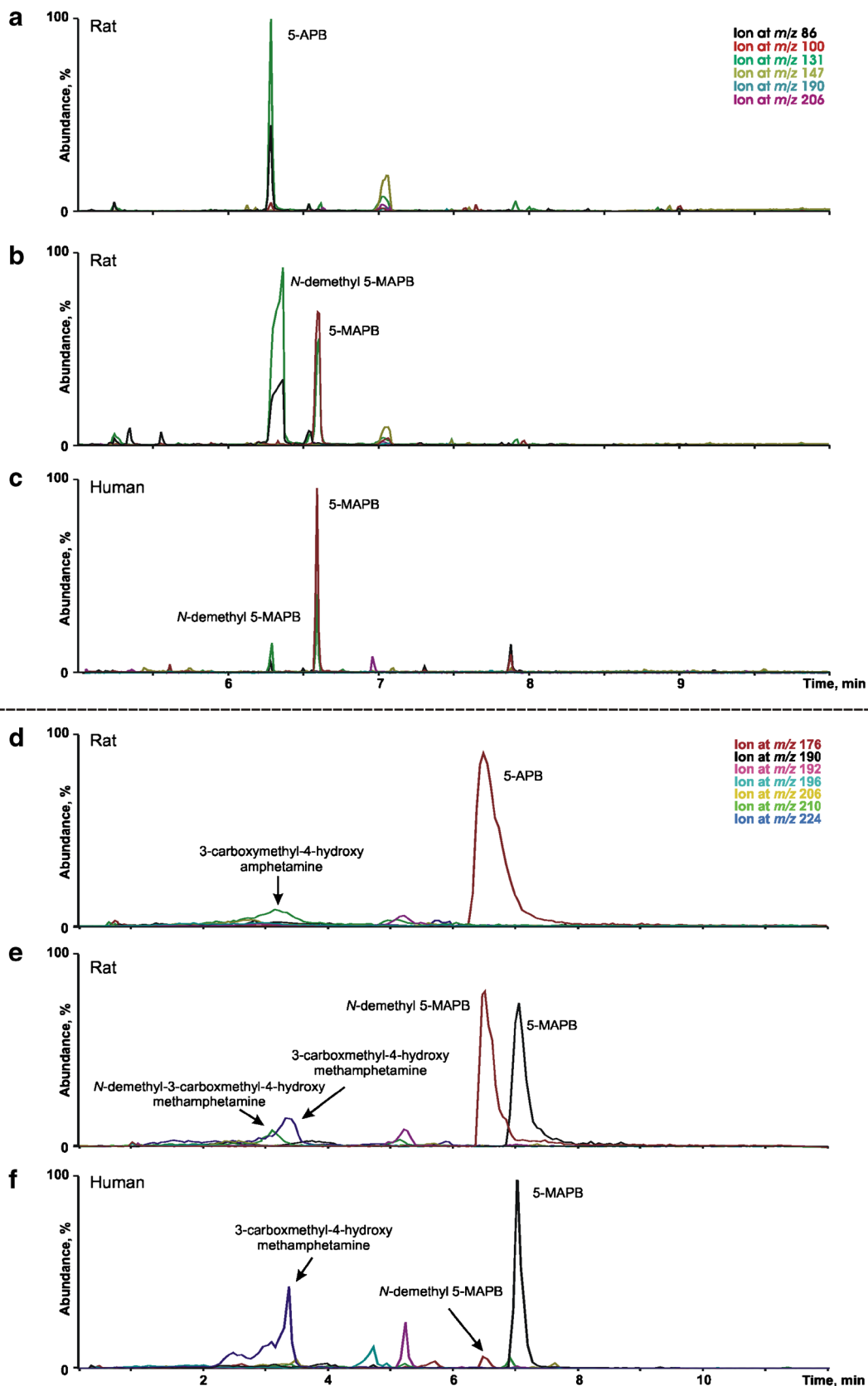
Fig. 4 Reconstructed ion chromatograms with the given ions from rat urines after a low dose of 5-APB (**a**), 5-MAPB (**b**), and from human urine after an unknown dose of 5-MAPB (**c**) after acid hydrolysis, liquid–liquid extraction and acetylation, and analysis with the GC-MS standard urine screening approach SUSA and after protein precipitation of those urines (**d–f**) and analysis with the LC-MS^n SUSA

of MDMA and MBDB (2-methylamino-1(3,4-methylendioxyphenyl)butane [30, 31]. Therefore, one should keep in mind that interactions cannot be excluded between strong CYP2B6 inhibitors (e.g., ticlopidine) and 5-MAPB, which might lead to side effects after a common dose because of increased plasma concentrations.

Toxicological detection of 5-APB and 5-MAPB by GC-MS or LC-MS^n

Using the GC-MS-based SUSA [9, 15], an intake of the compounds could be monitored in rat urine after administration of 3 mg/kg BM 5-APB or 1 mg/kg BM 5-MAPB, respectively. These doses corresponded to reported oral human single doses of about 30 mg for 5-APB or 10 mg for 5-MAPB scaled by dose-by-factor approach according to Sharma et al. [32]. Therefore, detection of the intake of these compounds should be possible also in human urine. The possible presence of 5-APB or 5-MAPB and their metabolites, within the GC-MS SUSA, were indicated by reconstructed mass chromatography with the ions at m/z 58, 86, 100, 131, 147, 160, 163, 174, 190, 206, and 218 for acetylated 5-APB, 5-MAPB, and their hydroxy, 3-hydroxyethyl-4-hydroxy or hydroxy, 3-carboxymethyl-4-hydroxy metabolites according to the corresponding reference spectra given in Fig. 1.

Figure 4 upper part shows reconstructed ion chromatograms from rat urine after a low dose of 5-APB (a), 5-MAPB (b), and a human urine sample after an unknown dose of 5-MAPB (c). As can be seen in the low-dose rat urine 5-APB, 5-MAPB and the corresponding N-demethyl 5-MAPB were the most abundant analytes and thus the targets for screening. Furthermore, investigation of the human urine samples showed that after ingestion of 5-MAPB, at least 5-MAPB itself could be detected along with N-demethyl 5-MAPB, which was in line with the in vivo rat urine results. Therefore, the assay should be suitable for drug testing in human urine, although the ingested amount of 5-MAPB was not known. The other metabolites may also occur in human urine in case of severe overdose and/or genetic variations of metabolism, and thus, they should be included in the mass chromatograms. Confirmation of the identity of the peaks indicated by the selected mass chromatogram was performed by computerized comparison of the underlying full-scan mass spectrum with reference spectra recorded during this study. Additionally, the full scan data files acquired by the GC-MS system were evaluated by AMDIS allowing the detection of 5-APB or 5-MAPB in the prepared urine samples using the previously described procedure [16].

Using the LC-MS^n SUSA, only 5-APB (1) and 3-carboxymethyl-4-hydroxy amphetamine (5) could be detected
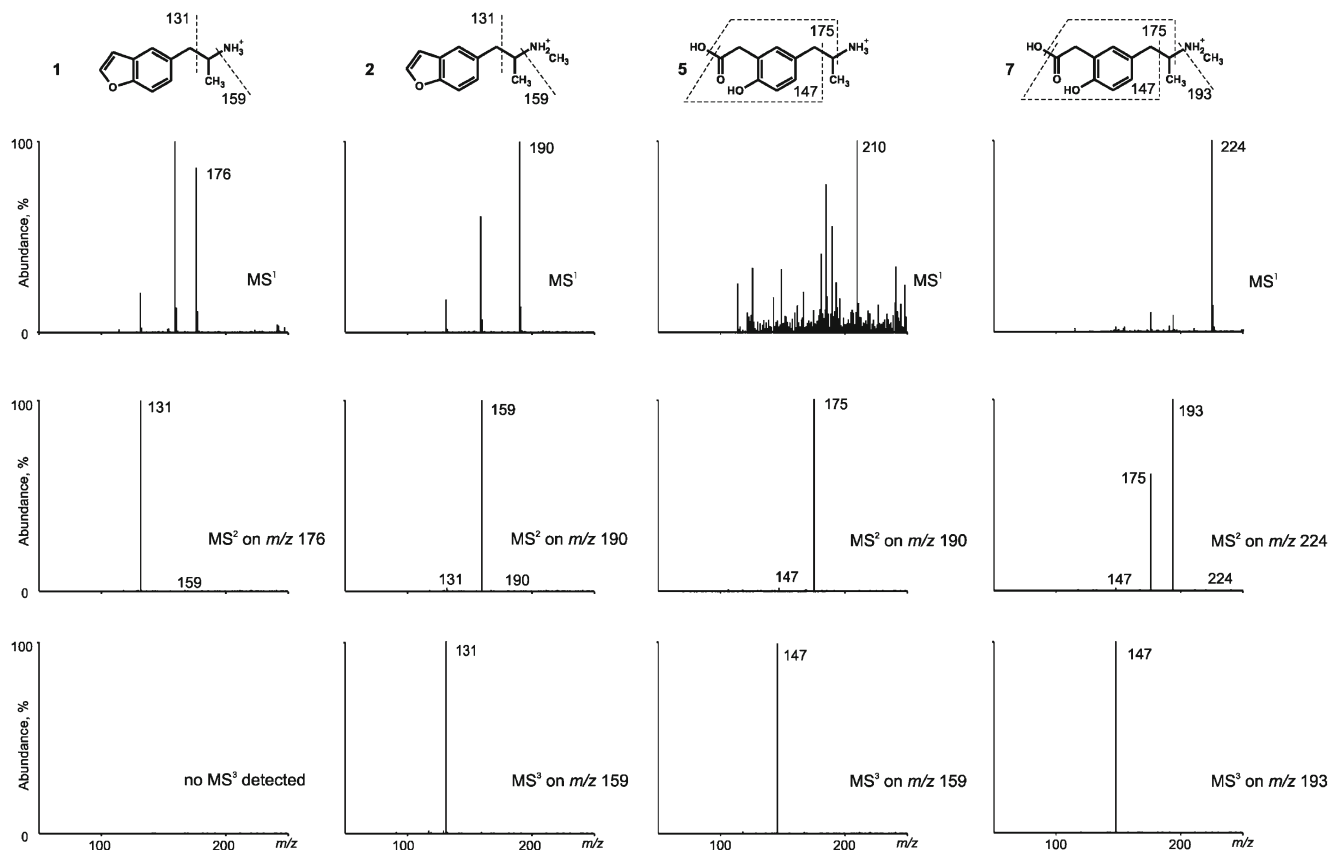
Fig. 5 Structures, proposed fragmentation patterns, MS^1, MS^2, and MS^3 spectra of 5-APB (*1*), 5-MAPB (*2*), 3-carboxymethyl-4-hydroxy amphetamine (*5*), and 3-carboxymethyl-4-hydroxy methamphetamine (*7*) after protein precipitation of urine samples and analysis with the LC-MS^n SUSA

in the 5-APB low-dose rat urine. For 5-MAPB (2), N-demethyl 5-MAPB (1), 3-carboxymethyl-4-hydroxy methamphetamine (7), and N-demethyl-3-carboxymethyl-4-hydroxy amphetamine (5) could be detected in rat urine. Similar results were observed in the human urine samples after ingestion of 5-MAPB. At least 5-MAPB could be detected, even if the drug was taken days before. In the case of recent ingestion, N-demethyl 5-MAPB and 3-carboxymethyl-4-hydroxy methamphetamine (7) could be detected additionally. Figure 4 lower part shows ion chromatograms reconstructed after the full-scan acquisition of rat urine after a low dose of 5-APB (d), 5-MAPB (e), and a human urine after an unknown dose of 5-MAPB (f). Although the parent compounds did not show characteristic fragmentation patterns without prior acetylation, it was possible to confirm the intake of 5-APB or 5-MAPB at least via the spectrum of the unchanged drug, the 3-carboxymethyl-4-hydroxy metabolites, and retention times. Figure 5 shows the corresponding MS^1, MS^2, and MS^3 spectra for 5-APB (1), 5-MAPB (2), 3-carboxymethyl-4-hydroxy amphetamine (5), and 3-carboxymethyl-4-hydroxy methamphetamine (7) with the corresponding chemical structures.

Quantification of 5-APB and 5-MAPB in plasma

The quantification method was validated according to Peters et al. as recommended for single case analysis [18]. Selectivity, linearity, accuracy, precision, and LOQ were tested. Accuracy was 91.1 % for the low and 95.5 % for the high concentration and precision data were 9.4 and 11.8 % for the low and the high concentration, respectively. The LOQ was consistent with the lowest calibrator and within the required acceptance criteria. The plasma concentrations determined in six clinical cases ranged from 5 to 124 µg/L for 5-MAPB and from 1 to 38 µg/L for its N-demethyl metabolite 5-APB. Considering similar doses as described on drug users' internet forums, these concentrations are comparable to published data for MDMA (1–514 µg/L) and MDA (1–67 µg/L) [28, 33].

Conclusions

The presented study showed that 5-APB and 5-MAPB were metabolized only to a minor extent. CYP1A2, CYP2B6, CYP2C19, and CYP2D6 were capable of catalyzing the N-demethylation of 5-MAPB. For CYPB6 and CYP2D6 the kinetic profiles follow Michaelis–Menten kinetics whereas the kinetic profiles for CYP1A2 and CYP2C19 show substrate inhibition. Both SUSAs were suitable to prove an intake of each drug in urine focusing on the detection of the parent

drugs and for 5-MAPB also on the N-demethyl metabolite. Authentic human 5-MAPB samples showed plasma concentrations in the same range as described for MDMA and its metabolite MDA.

References

1. Advisory Council on the Misuse of Drugs (ACMD) (2013) Benzofurans: a review of the evidence of use and harm. https://www.gov.uk/government/uploads/system/uploads/attachment_data/file/261783/Benzofuran_compounds_report pdf
2. Iversen L, Gibbons S, Treble R, Setola V, Huang XP, Roth BL (2013) Neurochemical profiles of some novel psychoactive substances. Eur J Pharmacol 700:147–151
3. Dawson P, Opacka-Juffry J, Moffatt JD, Daniju Y, Dutta N, Ramsey J, Davidson C (2014) The effects of benzofury (5-APB) on the dopamine transporter and 5-HT2-dependent vasoconstriction in the rat. Prog Neuropsychopharmacol Biol Psychiatry 48:57–63
4. Stanczuk A, Morris N, Gardner EA, Kavanagh P (2013) Identification of (2-aminopropyl)benzofuran (APB) phenyl ring positional isomers in internet purchased products. Drug Test Anal 5: 270–276
5. Casale JF, Hays PA (2012) The characterization of 6-(2-aminopropyl)benzofuran and differentiation from its 4-, 5-, and 7-positional analogues. Microgram J 9:61–74
6. Maurer HH, Pfleger K, Weber AA (2011) Mass spectral library of drugs, poisons, pesticides, pollutants and their metabolites. Wiley-VCH, Weinheim
7. Wissenbach DK, Meyer MR, Remane D, Weber AA, Maurer HH (2011) Development of the first metabolite-based LC-MSn urine drug screening procedure—exemplified for antidepressants. Anal Bioanal Chem 400:79–88
8. Maurer HH, Wissenbach DK, Weber AA (2014) Maurer/Wissenbach/Weber MWW LC-MSn library of drugs, poisons, and their metabolites. Wiley-VCH, Weinheim
9. Welter J, Meyer MR, Wolf E, Weinmann W, Kavanagh P, Maurer HH (2013) 2-Methiopropamine, a thiophene analogue of methamphetamine: studies on its metabolism and detectability in the rat and human using GC-MS and LC-(HR)-MS techniques. Anal Bioanal Chem 405:3125–3135
10. Dinger J, Meyer MR, Maurer HH (2014) Development and validation of a liquid-chromatography high-resolution tandem mass spectrometry approach for quantification of nine cytochrome P450 (CYP) model substrate metabolites in an in vitro CYP inhibition cocktail. Anal Bioanal Chem 406:4453–4464
11. Meyer MR, Vollmar C, Schwaninger AE, Maurer HH (2012) New cathinone-derived designer drugs 3-bromomethcathinone and 3-fluoromethcathinone: studies on their metabolism in rat urine and human liver microsomes using GC-MS and LC-high-resolution MS and their detectability in urine. J Mass Spectrom 47:253–262
12. Crespi CL, Miller VP (1999) The use of heterologously expressed drug metabolizing enzymes—state of the art and prospects for the future. Pharmacol Ther 84:121–131
13. Venkatakrishnan K, von Moltke LL, Court MH, Harmatz JS, Crespi CL, Greenblatt DJ (2000) Comparison between cytochrome P450 (CYP) content and relative activity approaches to scaling from cDNA-expressed CYPs to human liver microsomes: ratios of

accessory proteins as sources of discrepancies between the approaches. Drug Metab Dispos 28:1493–1504

14. Grime K, Riley RJ (2006) The impact of in vitro binding on in vitro-in vivo extrapolations, projections of metabolic clearance and clinical drug–drug interactions. Curr Drug Metab 7:251–264

15. Maurer HH, Pfleger K, Weber AA (2011) Mass spectral and GC data of drugs, poisons, pesticides, pollutants and their metabolites. Wiley-VCH, Weinheim

16. Meyer MR, Peters FT, Maurer HH (2010) Automated mass spectral deconvolution and identification system for GC-MS screening for drugs, poisons, and metabolites in urine. Clin Chem 56:575–584

17. Peters FT, Schaefer S, Staack RF, Kraemer T, Maurer HH (2003) Screening for and validated quantification of amphetamines as well as of amphetamine- and piperazine-derived designer drugs in human blood plasma by gas chromatography–mass spectrometry. Proceedings of the XIIIth GTFCh Symposium in Mosbach Proceedings of the XIIIth GTFCh Symposium in Mosbach: 323–333

18. Peters FT, Drummer OH, Musshoff F (2007) Validation of new methods [review]. Forensic Sci Int 165:216–224

19. McLafferty FW, Turecek F (1993) Interpretation of mass spectra. University Science Books, Mill Valley

20. Smith RM, Busch KL (1999) Understanding mass spectra—a basic approach. Wiley, New York

21. Connelly JC, Connor SC, Monte S, Bailey NJ, Borgeaud N, Holmes E, Troke J, Nicholson JK, Gavaghan CL (2002) Application of directly coupled high performance liquid chromatography-NMR-mass spectrometry and 1H NMR spectroscopic studies to the investigation of 2,3-benzofuran metabolism in Sprague-Dawley rats. Drug Metab Dispos 30:1357–1363

22. Kobayashi T, Sugihara J, Harigaya S (1987) Mechanism of metabolic cleavage of a furan ring. Drug Metab Dispos 15:877–881

23. Le Fur JM, Labaune JP (1985) Metabolic pathway by cleavage of a furan ring. Xenobiotica 15:567–577

24. Dalvie DK, Kalgutkar AS, Khojasteh-Bakht SC, Obach RS, O'Donnell JP (2002) Biotransformation reactions of five-membered aromatic heterocyclic rings. Chem Res Toxicol 15:269–299

25. Renzulli C, Nash M, Wright M, Thomas S, Zamuner S, Pellegatti M, Bettica P, Boyle G (2011) Disposition and metabolism of [14C]SB-649868, an orexin 1 and 2 receptor antagonist, in humans. Drug Metab Dispos 39:215–227

26. Ravindranath V, Burka LT, Boyd MR (1984) Reactive metabolites from the bioactivation of toxic methylfurans. Science 224:884–886

27. Ou T, Tatsumi K, Yoshimura H (1977) Isolation and identification of urinary metabolites of AF-2 (3-(5-nitro-2-furyl)-2-(2-furyl)acrylamide) in rabbits. Biochem Biophys Res Commun 75:401–405

28. Kraemer T, Maurer HH (2002) Toxicokinetics of amphetamines: metabolism and toxicokinetic data of designer drugs, of amphetamine, methamphetamine and their N-alkyl derivatives [review]. Ther Drug Monit 24:277–289

29. Meyer MR, Maurer HH (2010) Metabolism of designer drugs of abuse: an updated review [review]. Curr Drug Metab 11:468–482

30. Meyer MR, Peters FT, Maurer HH (2008) The role of human hepatic cytochrome P450 isozymes in the metabolism of racemic 3,4-methylenedioxy-methamphetamine and its enantiomers. Drug Metab Dispos 36:2345–2354

31. Meyer MR, Peters FT, Maurer HH (2009) Stereoselective differences in the cytochrome P450-dependent dealkylation and demethylation of N-methyl-benzodioxolyl-butanamine (MBDB, Eden) enantiomers. Biochem Pharmacol 77:1725–1734

32. Sharma V, McNeill JH (2009) To scale or not to scale: the principles of dose extrapolation. Br J Pharmacol 157:907–921

33. Hartman RL, Desrosiers NA, Barnes AJ, Yun K, Scheidweiler KB, Kolbrich-Spargo EA, Gorelick DA, Goodwin RS, Huestis MA (2014) 3,4-Methylenedioxymethamphetamine (MDMA) and metabolites disposition in blood and plasma following controlled oral administration. Anal Bioanal Chem 406:587–599